ChemComm

COMMUNICATION

View Article Online
View Journal | View Issue

Cite this: *Chem. Commun.*, 2025, **61**, 6957

Received 4th March 2025,
Accepted 9th April 2025

DOI: 10.1039/d5cc01194a

rsc.li/chemcomm

A highly active sulfur based pincer ruthenium catalyst for CO_2 hydrogenation†

Alexander Mondragón-Díaz,[a] Steven P. Kelley,[a] Nilay Hazari[b] and Wesley H. Bernskoetter*[a]

The synthesis of a new air-stable SPS pincer ligand that supports a Ru catalyst for CO_2 hydrogenation to formate is described. This rare S-donor based pincer system gives higher activity compared to related PNP supported Ru catalysts and is less dependent on Lewis acidic Li co-catalysts for achieving high turnover numbers. The SPS ligated Ru catalyst is also active for *N*-formylation of amines with CO_2.

Pincer ligands are commonly used to support homogeneous transition metal catalysts because of their electronic and structural versatility.[1] In particular, PNP type pincer ligands can support active catalysts for a plethora of transformations using metals from across the transition series.[2,3] For example, our own laboratories and others have employed group VIII complexes ligated with PNP pincer ligands as catalysts for CO_2 hydrogenation and related processes.[4–6] While the steric and electronic properties of PNP ligands are frequently modified by varying the phosphine substituents,[7–9] this is often synthetically challenging. Further, PNP ligands can be air-sensitive and typically their syntheses require expensive precursors. In principle, replacing the phosphine donors in PNP ligands with weaker σ-donating thioethers provides advantages in terms of ligand cost and improved air stability.[10,11] Nevertheless, examples of pincer ligands with sulfur donors are limited. Recent studies of S-donor analogues of widely utilized Ru-MACHO PNP and Ru-pyridyl PNP catalysts report inferior catalytic performance compared to PNP ligated complexes, likely because the Ru centers are less electron rich and have significantly higher reduction potentials.[10a,12] To address this issue, in our current study we have a prepared a new air-stable P- and S-donor hybrid pincer ligand, $CH_3P(C_6H_4S^tBu)_2$ ($^{tBu}SP^{Me}S$), and used it to develop an SPS Ru dihydride catalyst, ($^{tBu}SP^{Me}S$)Ru(PPh_3)H_2, for CO_2 hydrogenation and amine formylation. This catalyst displays superior CO_2 hydrogenation activity compared to related PNP Ru systems. Preliminary mechanistic studies identified an SPS Ru formate hydride complex as the likely resting state in catalytic CO_2 reduction.

We hypothesized that a SPS pincer ligand would be more electron rich than a SNS pincer ligand and potentially give comparable reactivity to PNP ligated complexes. Therefore, we targeted $^{tBu}SP^{Me}S$, which contains a strongly donating central P-donor, alongside two S-donors, with sterically bulky ^{t}Bu-substituents to prevent dimerization. $^{tBu}SP^{Me}S$ was prepared in three high yielding steps from inexpensive and commercially available starting materials (Scheme 1).[13] Initially 2-bromothiophenol was converted into (2-bromophenyl)(*tert*-butyl)sulfane, which was treated with ^{n}BuLi and PCl_3 to form $^{tBu}SP^{Cl}S$. Reaction of $^{tBu}SP^{Cl}S$ with methyl Grignard generated the $^{tBu}SP^{Me}S$ ligand. Notably, benzene solutions of $^{tBu}SP^{Me}S$ are stable to air at ambient temperature for more than one week.

Starting from commercially available $[Ru(PPh_3)_3]Cl_2$, the Ru dichloride complex ($^{tBu}SP^{Me}S$)Ru(PPh_3)Cl_2 (**1-Cl$_2$**) was prepared in nearly quantitative yield by ligand substitution over 1 h at ambient temperature (Scheme 2). The ^{1}H NMR spectrum of the isolated yellow solid displays one doublet at 0.82 ppm for the P–(CH_3) group, and two equal intensity resonances for the S–^{t}Bu groups at 1.75 and 0.90 ppm, consistent with two thioethers groups occupying distinct chemical environments. These are consistent with X-ray diffraction studies of **1-Cl$_2$** that indicate the $^{tBu}SP^{Me}S$ ligand is bound in a *fac* mode with thioether groups positioned *trans* to the Cl and PPh_3 ligands (Fig. 1, left). The PPh_3 ligand in **1-Cl$_2$** is oriented *cis* to the P-donor of the $^{tBu}SP^{Me}S$, in agreement with the two doublets at δ 86.72 and δ 28.55 ppm observed in the $^{31}P\{^1H\}$ NMR spectrum. The *fac*-ligation of the pincer ligand in **1-Cl$_2$** contrasts with

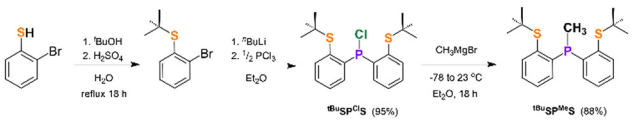

Scheme 1 Synthesis of the $^{tBu}SP^{Me}S$ ligand.

[a] *Department of Chemistry, University of Missouri, Columbia, MO, USA. E-mail: bernskoetterwh@missouri.edu*
[b] *Department of Chemistry, Yale University, New Haven, CT, USA*

† Electronic supplementary information (ESI) available. CCDC 2427581–2427583. For ESI and crystallographic data in CIF or other electronic format see DOI: https://doi.org/10.1039/d5cc01194a

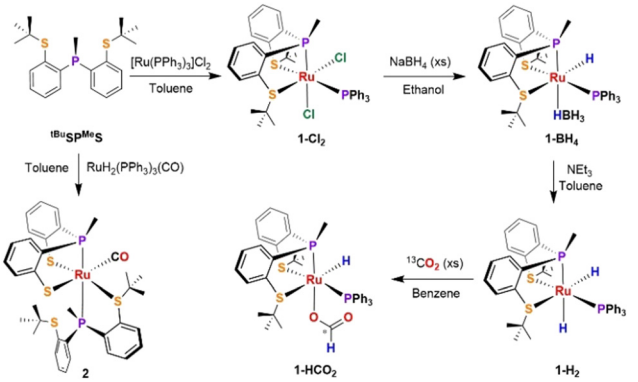

Scheme 2 Synthesis of the [(^{tBu}SP^{Me}S)Ru] complexes **1-Cl$_2$**, **1-BH$_4$**, **1H$_2$**, **1-CO$_2$H** and **2**.

most reported PNP and SNS Ru complexes, which bind in a *mer* orientation.[2e,10b,12b]

Treatment of **1-Cl$_2$** with $NaBH_4$ in EtOH initially afforded a species tentatively identified as (^{tBu}SP^{Me}S)Ru(PPh$_3$)(H)(BH$_4$) (**1-BH$_4$**) which exhibited a ^{1}H NMR spectrum containing a Ru–H resonance at δ −13.05 ppm (dd, $^2J_{P-H}$ = 29, 23 Hz) integrating to one proton, as well as a broad resonance centered at δ −0.80 ppm, integrating to four protons (Scheme 2). This signal is similar to those observed for other rapidly exchanging M–BH$_4$ complexes.[3d,4a,6a,14a] Exposure of **1-BH$_4$** to low pressures or standing under N_2 at ambient temperature for 1 h resulted in partial conversion to the corresponding Ru dihydride complex, (^{tBu}SP^{Me}S)Ru(PPh$_3$)H$_2$ (**1-H$_2$**), obviating isolation of pure samples of **1-BH$_4$**. **1-H$_2$** was obtained in 90% yield by treatment of toluene solutions of **1-BH$_4$** with triethylamine over 4 h (Scheme 2). The ^{1}H NMR spectrum of **1-H$_2$** in C_6D_6 displays two sets of 8-line resonances consistent with Ru–H ligands bound *cis* (−12.04 ppm) and *trans* (−5.05 ppm) to the P-atom in ^{tBu}SP^{Me}S.[14] The molecular structure of **1-H$_2$** was confirmed by X-ray diffraction (Fig. 1, center). The ^{tBu}SP^{Me}S ligand is again bound in a *fac* geometry with two Ru–H moieties located in a mutually *cis* arrangement, consistent with the solution NMR data. The Ru–H bond lengths differ significantly, with Ru(1)–H(1) approximately 0.16 Å longer than Ru(1)–H(2) owing to the strongly σ-donating properties of the phosphorus donor compared with the thioether donor. Significantly, these differences in Ru–H bond length impact the relative nucleophilic activity of these hydride ligands and lead to a marked difference in their tendency to undergo insertion reactions (*vide infra*).[15]

Pincer ligated Ru hydride complexes are leading catalysts for carbonyl reduction,[4b,c,e,5,9] which motivated our evaluation of **1-H$_2$** for catalytic CO_2 hydrogenation. Using conditions previously optimized for (^{iPr}PN^{R}P)RuHCl(CO) (^{iPr}PN^{R}P = [RN(CH$_2$CH$_2$P^{i}Pr$_2$)$_2$] R = H, Me or Ph),[5a] 0.3 μmol of **1-H$_2$** under 500 psi H_2/CO_2 (1 : 1) in the presence of excess 1,8-diazabicyclo[5.4.0]undec-7-ene (DBU) resulted in the hydrogenation of CO_2 to formate (Table 1). After 1 h, **1-H$_2$** produced formate with a turnover number (TON) of 5600 (entry 1), demonstrating an activity roughly 10 times higher than that of (^{iPr}PN^{Me}P)Ru(H)$_2$(CO) and 6 times greater than (^{iPr}PN^{H}P)Ru(H)$_2$(CO) under comparable conditions.[5a] The TON at this short interval is determined largely by the initial rate of catalysis and serves as an approximation of the turnover frequency (TOF) for **1-H$_2$**. Our results indicate that air stable S-donor pincer ligands can provide superior catalytic performance compared to state-of-the-art PNP ligands.[5a] Excellent catalytic activity was also observed for **1-H$_2$** in the presence of co-catalytic amounts of lithium triflate (LiOTf) (1.5 mmol) and a TON of 15 700 was observed after 1 h (entry 2). The beneficial effects of Lewis acids (LAs), such as LiOTf, in CO_2 hydrogenation reactions has been observed in many related pincer-supported systems for CO_2 hydrogenation.[4e,5a,16] Extending reaction times to 6 h narrows the gap in catalytic productivity between trials with and without LA (entries 3 & 4). After 24 h, the enhancing effects of LiOTf are minor (entries 5 & 6), with experiments using only **1-H$_2$** achieving a TON of over 30 000. In fact, there is essentially no increase in TON between 6 h and 24 h in the presence of LiOTf, suggesting the catalyst is largely deactivated after 6 h. In the absence of LiOTf, the catalyst is active up to 24 h, with no increase between 24 h and 48 h (entry 7). These trends suggest that while LiOTf, a common co-catalyst for these reactions,

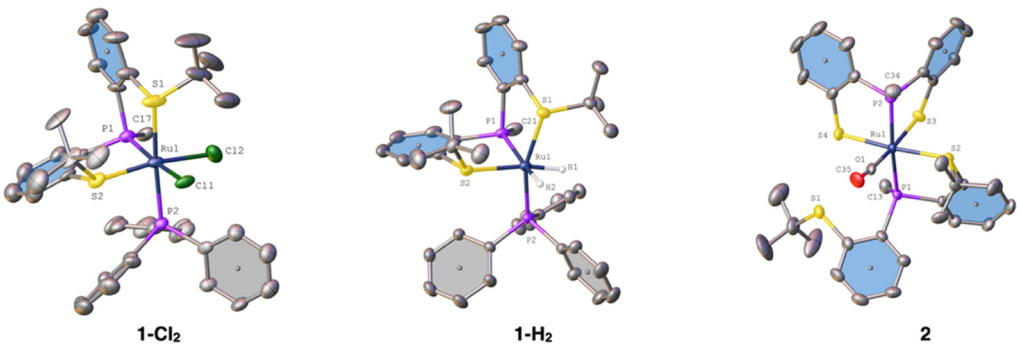

Fig. 1 Solid State structure of **1-Cl$_2$** (left), **1-H$_2$** (center) and **2** (right). Thermal ellipsoids are shown at 50% probability. Hydrogen atoms, solvent molecules are omitted for clarity. Selected bond lengths (Å) and angles (deg) for **1-Cl$_2$**: Ru(1)–P(1) 2.213(2), Ru(1)–P(2) 2.366(2), Ru(1)–S(1) 2.430(2), Ru(1)–S(2) 2.344(2), Ru(1)–Cl(1) 2.505(2), Ru(1)–Cl(2) 2.453(2); P(1)–Ru(1)–P(2) 100.24(6), S(1)–Ru(1)–S(2) 96.46(7), Cl(1)–Ru(1)–Cl(2) 95.25(6), P(1)–Ru(1)–Cl(1) 170.29(7), **1-H$_2$**: Ru(1)–P(1) 2.262(6), Ru(1)–P(2) 2.263(6), Ru(1)–S(1) 2.373(7), Ru(1)–S(2) 2.399(7), Ru(1)–H(1) 1.500(5), Ru(1)–H(2) 1.650(5); P(1)–Ru(1)–P(2) 100.17(3), S(1)–Ru(1)–S(2) 101.95(2), H–Ru(1)–H(A) 87.00(3), P(1)–Ru(1)–H(A) 168.29(2), S(1)–Ru(1)–P(2) 160.40(3), S(2)–Ru(1)–H 172.00(2), P(1)–Ru(1)–H(A) 168.00(2).for **2**: Ru(1)–P(1) 2.366(1), Ru(1)–P(2) 2.302(1), Ru(1)–S(2) 2.391(1), Ru(1)–S(3) 2.458(1), Ru(1)–S(4) 2.395(1), Ru(1)–C(35) 1.858(5); P(1)–Ru(1)–P(2) 167.98(4), S(3)–Ru(1)–S(4) 90.95(4), S(4)–Ru(1)–S(2) 171.05(4), C(36)–Ru(1)–S(3) 175.20(2).

Table 1 CO_2 hydrogenation to formate catalyzed by **1-H$_2$**[a]

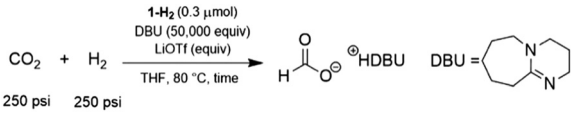

Entry	LiOTf (mmol)	T (°C)	Time (h)	TON[b]	Yield[c] (%)
1	0	80	1	5600 (600)	10
2	1.5	80	1	15 700 (1000)	32
3	0	80	6	22 000 (600)	44
4	1.5	80	6	34 500 (200)	69
5	0	80	24	30 200 (200)	60
6	1.5	80	24	34 000 (1000)	68
7	0	80	48	32 800 (1300)	66
8[d]	0	80	24	160 000 (10 000)	32
9[d]	1.5	80	24	105 000 (5000)	21

[a] Reaction conditions: 250 psi of CO_2/250 psi of H_2, **1-H$_2$** (0.3 μmol), DBU (2.34 g, 15.0 mmol), THF (10 mL), 80 °C. [b] TONs were quantified using ^{1}H NMR spectroscopy with DMF as an internal standard; reported values are the average of three trials with the standard deviation in parentheses. [c] The yield is based on DBU. [d] **1-H$_2$** = 0.03 μmol.

enhances the already leading activity of **1-H$_2$**, additives are not required to achieve high productivity and that LAs may accelerate catalyst deactivation in addition to improving the rate of formate production. This hypothesis is further supported by experiments with lower catalyst loadings (0.03 μmol) which achieve a maximum TON of 160 000 without LiOTf (entry 8). This corresponds to an average TOF of 6600 h^{-1} over the first 24 h of reaction time. In the presence of LiOTf these values decrease to a TON of 105 000 and an average TOF of 4400 h^{-1} (entry 9). Comparing TOF values between catalysts is often complicated by variation in reaction conditions and the length of time reactions are performed. Nevertheless, **1-H$_2$** delivers activity which is clearly higher than the most comparable Ru-MACHO PNP frameworks,[5a] though initial TOF values in excess of 1×10^6 h^{-1} have been reported for Ru-pyridyl PNP catalysts in CO_2 hydrogenation to formate.[4c]

To study the pathway of formate production, a sample of **1-H$_2$** was exposed to $^{13}CO_2$ and the reaction monitored by NMR spectroscopy. Spectra collected immediately following gas addition indicated complete conversion to a Ru formate hydride complex, [(^{tBu}SP^{Me}S)RuH(PPh$_3$)(HCO$_2$)] (**1-HCO$_2$**) (Scheme 2). The $^{13}CO_2$ derived formate ligand appears as a doublet at 8.92 ppm in the ^{1}H NMR with a corresponding resonance at 169.0 ppm in the ^{13}C NMR spectrum. Multinuclear 1D and 2D NMR studies indicate that the formate group is coordinated *trans* to the P atom of the ^{Bu}SP^{Me}S ligand, consistent with insertion occurring at the Ru–H opposite the more *trans* influencing phosphine site. Analysis after several days under $^{13}CO_2$ or at elevated temperatures up to 80 °C gave no indication of insertion into the remaining Ru–H of **1-HCO$_2$**. Unfortunately, isolation of **1-HCO$_2$** in pure form was not possible as exposure to vacuum caused immediate reversion to **1-H$_2$**, similar to reports of related Fe and Ru formate complexes.[5a] Previously, our laboratories and others have identified the insertion of CO_2 into Ru–H or Fe–H bonds as a key step in the catalytic hydrogenation of CO_2 to formate.[4a,5a,15,17] *In situ* NMR experiments starting from **1-H$_2$** under modified catalytic conditions (1 : 3 : 40 of **1-H$_2$** : $LiBF_4$: DBU in THF-d_8 under 2 atm of CO_2/H_2 at 23 °C) indicate **1-HCO$_2$** is the primary Ru complex present during formate production (Fig. S26, ESI†), consistent with **1-HCO$_2$** acting as the catalytic resting state. This suggests that loss of the formate ligand is the turnover limiting step in catalysis.

Many leading pincer supported Ru and Fe catalysts for carbonyl hydrogenation reactions contain CO ancillary ligands.[3d–5] The presence of these π-acids have been variously postulated to influence the *fac*/*mer* coordination mode of the pincer ligand, improve the stability of the catalysts and attenuate the steric and electronic properties of the metal.[18] Seeking to develop a CO coordinated analog of **1-H$_2$**, we attempted ligand substitution of PPh_3. However, exposure of **1-H$_2$** to CO gave no reaction at ambient temperature and led to unselective reactivity at elevated temperatures. Alternatively, treating [RuH$_2$(PPh$_3$)$_3$(CO)] with ^{tBu}SP^{Me}S in toluene at 100 °C resulted in the formation of a single SPS pincer containing product, [(κ^3-SP^{Me}S)Ru(κ^2-^{tBu}SP^{Me}S)(CO)] (**2**) (Scheme 2), in moderate yield based on the 2 : 1 SPS to Ru stoichiometry. Complex **2** is the result of two C–S bond activations of the ligand S–^{t}Bu groups and κ^2 coordination of an additional equivalent of ^{tBu}SP^{Me}S. The identity of the S–^{t}Bu derived organic products has remained elusive, but **2** was characterized by NMR and XRD analysis (Fig. 1, right). Catalytic trials using **2** indicate it is largely inactive for CO_2 hydrogenation (Table S1, ESI†), suggesting that activation of S-donor substituents in the presence of Ru–H groups may present a path toward catalyst deactivation. Analogous ligand activation reactions are rare for PNP complexes and should be carefully considered in the design of S-donor pincer ligands.

Metal-catalyzed formylation of amines with CO_2 and H_2 is another application of CO_2 hydrogenation which provides valuable chemicals.[19,20] A preliminary investigation into *N*-formylation using pyrrolidine was conducted using 0.2 mol% of **1-H$_2$** under 500 psi of H_2/CO_2 (1 : 1) at 120 °C for 24 h. A 96% yield of 1-formylpyrrolidine corresponding to a TON of 480 was observed (Fig. 2). A preliminary screening of other secondary and primary amine substrates revealed only modest activity and scope for this reaction (Table S3, ESI†). Reducing the loading of **1-H$_2$** to 0.002 mol% increased TON significantly to 4080, albeit with a yield decreased to 8%. Still, the activity of **1-H$_2$** towards CO_2 based *N*-formylation indicates that SPS or other S-donor pincer ligands are viable scaffolds for the development of new catalysts for other carbonyl reduction processes.

In summary, this work identifies a new, air stable SPS pincer ligand that can support a highly active and productive Ru catalyst for CO_2 hydrogenation to formate. The SPS-ligated Ru catalyst surpasses the activity of related PNP ligated Ru catalysts for CO_2 reduction and is less dependent on Lewis acidic LiOTf co-catalyst for achieving maximum productivity. Preliminary mechanistic studies suggest that CO_2 insertion into the strongly

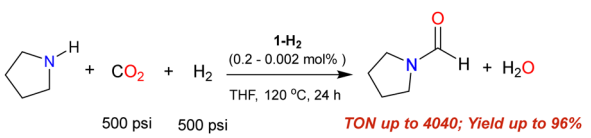

Fig. 2 *N*-Formylation of pyrrolidine with H_2 and CO_2 catalyzed by **1-H$_2$**.

trans influenced Ru–H of **1-H$_2$** produces a formate complex **1-HCO$_2$** that likely serves as the catalyst resting state. Attempts to incorporate a CO ancillary ligand into the coordination sphere of a SPS-ligated Ru complex resulted in deleterious C–S activation and formation of a poorly active Ru thiolate complex. This work provides rare examples of S-donor congeners of widely used PNP-ligated Ru hydrogenation catalysts and demonstrates the potential for enhancing catalytic performance with S-donor pincer ligands. Our laboratories are currently seeking to elucidate the origins for the improved catalyst performance, characterize deactivation pathways, and design superior air stable S-donor pincer ligand platforms.

Data availability

The experimental details supporting this article have been included as part of the ESI.† CCDC numbers 2427581–2427583 contain supplementary crystallographic data for **1-Cl$_2$**, **1-H$_2$**, and **2**.

Conflicts of interest

There are no conflicts to declare.

Notes and references

1 (*a*) L. González-Sebastián, A. Reyes-Sanchez and D. Morales-Morales, *Organometallics*, 2023, **42**, 2426–2446; (*b*) M. Esfandiari, G. Mohammadnezhad, O. Akintola, F. Otto, T. Fritz and W. Plass, *Dalton Trans.*, 2023, **52**, 11875–11885; (*c*) S. Martínez-Vivas, D. G. Gusev, M. Poyatos and E. Peris, *Angew. Chem., Int. Ed.*, 2023, **62**, e2023138.

2 (*a*) T. Mitsumoto, Y. Ashida, K. Arashiba, S. Kuriyama, A. Egi, H. Tanaka, K. Yoshizawa and Y. Nishibayashi, *Angew. Chem., Int. Ed.*, 2023, **62**, e2023066; (*b*) B. Wang, C. Rong, M. Lei, S. Liu and F. De Proft, *Inorg. Chem.*, 2023, **62**(19), 7366–7375; (*c*) Y. Liu, X. Yue, L. Li, Z. Li, L. Zhang, M. Pu, Z. Yang, C. Wang, J. Xiao and M. Lei, *Inorg. Chem.*, 2020, **59**(12), 8404–8411; (*d*) L. Alig, M. Fritz and S. Schneider, *Chem. Rev.*, 2019, **119**, 2681–2751; (*e*) A. Friedrich, M. Drees, M. Käss, E. Herdtweck and S. Schneider, *Inorg. Chem.*, 2010, **49**, 5482–5494.

3 (*a*) P. Hermosilla, P. López, P. García-Orduña, F. J. Lahoz, V. Polo and M. A. Casado, *Organometallics*, 2018, **37**(15), 2618–2629; (*b*) S. Kar and D. Milstein, *Chem. Commun.*, 2022, **58**, 3731–3746; (*c*) A. V. Zabula, Y. Qiao, A. J. Kosanovich, T. Cheisson, B. C. Manor, P. J. Carroll, O. V. Ozerov and E. J. Schelter, *Chem. – Eur. J.*, 2017, **23**, 17923–17934; (*d*) R. Langer, M. A. Iron, L. Konstantinovski, Y. Diskin-Posner, G. Leitus, Y. Ben-David and D. Milstein, *Chem. – Eur. J.*, 2012, **18**, 7196–7210.

4 (*a*) Y. Zhang, A. D. MacIntosh, J. L. Wong, E. A. Bielinski, P. G. Williard, B. Q. Mercado, N. Hazari and W. H. Bernskoetter, *Chem. Sci.*, 2015, **6**, 4291–4299; (*b*) R. Sen, A. Goeppert and G. K. S. Prakash, *Angew. Chem., Int. Ed.*, 2022, **61**, e202207278; (*c*) G. A. Filonenko, R. V. Putten, E. N. Schulpen, E. J. M. Hensen and E. A. Pidko, *ChemCatChem*, 2014, **6**, 1526–1530; (*d*) J. B. Curley, N. E. Smith, W. H. Bernskoetter, N. Hazari and B. Q. Mercado, *Organometallics*, 2018, **37**, 3846–3853; (*e*) W.-H. Wang, Y. Himeda, J. T. Muckerman, G. F. Manbeck and E. Fujita, *Chem. Rev.*, 2015, **115**, 12936–12973.

5 (*a*) J. B. Curley, C. Hert, W. H. Bernskoetter, N. Hazari and B. Q. Mercado, *Inorg. Chem.*, 2022, **61**, 643–656; (*b*) A. Agapova, E. Alberico, A. Kammer, H. Junge and M. Beller, *Chem. Cat. Chem.*, 2019, **11**, 1910–1914.

6 (*a*) E. Alberico, P. Sponholz, C. Cordes, M. Nielsen, H.-J. Drexler, W. Baumann, H. Junge and M. Beller, *Angew. Chem., Int. Ed.*, 2013, **52**, 14162–14166; (*b*) X.-F. Liu, X.-Y. Li and L.-N. He, *Eur. J. Org. Chem.*, 2019, 2437–2447; (*c*) Z. Chen, S. Du, J. Zhanga and X.-F. Wu, *Green Chem.*, 2020, **22**, 8169–8182.

7 (*a*) S. Lapointe, E. Khaskin, R. R. Fayzullin and J. R. Khusnutdinova, *Organometallics*, 2019, **38**(7), 1581–1594; (*b*) D. Benito-Garagorri and K. Kirchner, *Acc. Chem. Res.*, 2008, **41**(2), 201–213; (*c*) S. Gu, R. J. Nielsen, K. H. Taylor, G. C. Fortman, J. Chen, D. A. Dickie, W. A. Goddard III and T. B. Gunnoe, *Organometallics*, 2020, **39**(10), 1917–1933.

8 D. Benito-Garagorri, E. Becker, J. Wiedermann, W. Lackner, M. Pollak, K. Mereiter, J. Kisala and K. Kirchner, *Organometallics*, 2006, **25**(8), 1900–1913.

9 S. Kar, R. Sen, J. Kothandaraman, A. Goeppert, R. Chowdhury, S. B. Munoz, R. Haiges and G. K. S. Prakash, *J. Am. Chem. Soc.*, 2019, **141**, 3160–3170.

10 (*a*) D. N. Chirdon, S. P. Kelley, N. Hazari and W. H. Bernskoetter, *Organometallics*, 2021, **40**, 4066–4076; (*b*) C. Vinas, P. Angles, G. Sanchez, N. Lucena, F. Teixidor, L. Escriche, J. Casabo, J. F. Piniella, A. Alvarez-Larena, R. Kivekäs and R. Sillanpää, *Inorg. Chem.*, 1998, **37**, 701–707.

11 M. R. Elsby and R. T. Baker, *Acc. Chem. Res.*, 2023, **56**, 798–809.

12 (*a*) D. S. McGuinness, P. Wasserscheid, W. Keim, D. Morgan, J. T. Dixon, A. Bollmann, H. Maumela, F. Hess and U. Englert, *J. Am. Chem. Soc.*, 2003, **125**, 5272–5273; (*b*) D. Spasyuk, S. Smith and D. G. Gusev, *Angew. Chem.*, 2013, **125**, 2598–2602; (*c*) J. Schörgenhumer, A. Zimmermann and M. Waser, *Org. Process Res. Dev.*, 2018, **22**, 862–870.

13 (*a*) S. B. Harkins and J. C. Peters, *J. Am. Chem. Soc.*, 2004, **126**, 2885–2893; (*b*) Y.-E. Kim, J. Kim and Y. Lee, *Chem. Commun.*, 2014, **50**, 11458–11461.

14 (*a*) C. Bianchini, P. J. Perez, M. Peruzzini, F. Zanobini and A. Vacca, *Inorg. Chem.*, 1991, **30**, 279–287; (*b*) M. Hirano, S. Togashi, M. Ito, Y. Sakaguchi, N. Komine and S. Komiya, *Organometallics*, 2010, **29**, 3146–3159; (*c*) M. M. Bhadbhade, L. D. Field, R. Gilbert-Wilson, R. W. Guest and P. Jensen, *Inorg. Chem.*, 2011, **50**, 6220–6228; (*d*) P. Lorusso, G. R. Easthamb and D. J. Cole-Hamilton, *Dalton Trans.*, 2018, **47**, 9411–9417.

15 (*a*) Y.-Y. Ohnishi, T. Matsunaga, Y. Nakao, H. Sato and S. Sakaki, *J. Am. Chem. Soc.*, 2005, **127**, 4021–4032; (*b*) T. Liu, Z. Liu, L. Tang, J. Li and Z. Yang, *Catalysts*, 2021, **11**(1356), 1–10.

16 (*a*) L. Pavlovic and K. H. Hopmann, *Organometallics*, 2023, **42**, 3025–3035; (*b*) A. Maity and T. S. Teets, *Chem. Rev.*, 2016, **116**, 8873–8911.

17 (*a*) G. Liang and Min Zhang, *Chem. – Eur. J.*, 2024, **30**, e202402114; (*b*) S. Ramakrishnan, K. M. Waldie, I. Warnke, A. G. De Crisci, V. S. Batista, R. M. Waymouth and C. E. D. Chidsey, *Inorg. Chem.*, 2016, **55**, 1623–1632; (*c*) P. Zhang, S.-F. Ni and L. Dang, *Chem. – Asian J.*, 2016, **11**, 2528–2536.

18 (*a*) D. Benito-Garagorri, M. Puchberger, K. Mereiter and K. Kirchner, *Angew. Chem., Int. Ed.*, 2008, **47**, 9142–9145; (*b*) I. Koehne, T. J. Schmeier, E. A. Bielinski, C. J. Pan, P. O. Lagaditis, W. H. Bernskoetter, M. K. Takase, C. Würtele, N. Hazari and S. Schneider, *Inorg. Chem.*, 2014, **53**, 2133–2143; (*c*) N. E. Smith, W. H. Bernskoetter, N. Hazari and B. Q. Mercado, *Organometallics*, 2017, **36**, 3995–4004; (*d*) M. Halder, D. Castillo Cardenas, A. M. Chartouni and D. B. Culver, *Dalton Trans.*, 2025, **54**, 2851–2859.

19 (*a*) L. Zhang, Z. Han, X. Zhao, Z. Wang and K. Ding, *Angew. Chem., Int. Ed.*, 2015, **54**, 6186–6189; (*b*) U. Jayarathne, N. Hazari and W. H. Bernskoetter, *ACS Catal.*, 2018, **8**, 1338–1345; (*c*) M. Hulla, G. Laurenczy and P. J. Dyson, *ACS Catal.*, 2018, **8**, 10619–10630; (*d*) M. Rahman, I. Dutta, S. S. Gholap, G. N. Ngô, Y. Rachuri, L. Alrais and K.-W. Huang, *ChemCatChem*, 2024, **16**, e202401202.

20 (*a*) K. Weissermel and H.-J. Arpe, *Industrial Organic Chemistry*, Translated by C. R. Lindley, Wiley-VCH, Weinheim, 3rd edn, 1997; (*b*) H. Bipp and H. Kieczka, Formamides. *Ullmann's Encyclopedia of Industrial Chemistry*, Wiley-VCH, Weinheim, Germany, 2003, vol. 15, pp. 36–47.

